RESUME OF THE EXTENSION OF THE PONCHON AND SAVARIT METHOD FOR DESIGNING TERNARY RECTIFICATION COLUMNS

*from Juan A. Reyes-Labarta Doctoral Thesis: "**Design of Multicomponent Rectification and Extraction Columns. Minimum Reflux Calculation"**. ISBN: 84-699-5991-3

(http://www.cervantesvirtual.com/FichaObra.html?Ref=4845)

Chemical Engineering Department, University of Alicante, Apdo. 99, Alicante 03080, Spain

Tel. (34) 965 903861 Fax (34) 965 903826 E-mail: ja.reyes@ua.es

Abstract

This work presents a summary of the analytical extension of the classical Ponchon and Savarit method for the design of binary distillation columns to ternary systems. For a given feasible separation, convergence is almost always guaranteed in calculation times comparable to those used by commercial simulation packages. However, in this case the total number of stages and the optimal feed location are simultaneously determined. For ternary mixtures it is possible graphical representation keeping all the intuitive characteristics of the original method for binary mixtures.

The presented approach include the possibility of approximate (with interpolation, correlation and intersection methods) or rigorous calculations of mass and energy balances and equilibrium relations and the direct calculation of the minimum number of equilibrium stages and the optimum feed point location for a specific product separation with a specified reflux ratio. The distillate flow rate and the reflux ratio can be optimised in an outer loop providing the method a great flexibility.

Keywords: Distillation, tray-type separators, design, Ponchon and Savarit method, multicomponent mixtures.

1. Introduction

Distillation is the most important separation technique, even though it is an expensive operation in terms of capital and operating costs, and it is likely that distillation continues being the most important separation technique for a long time. So, distillation is one of the most studied unit operations.

From the very early stages of their education, Chemical engineers are able of design distillation columns for separating binary mixtures using, for example the classical methods of Sorel[1] or Ponchon-Savarit[2]. These methods solve alternatively the mass and energy balance (to relate the streams between stages) and the equilibrium equations (to relate the composition of the phases in equilibrium at each stage) to obtain the number of trays, the position of the feed stages, the composition in all trays, temperature profile and so on. It is a rigorous design method!. The great acceptance of these methods for educational purposes is due to the graphical approach used for solving the design problem -although a pure numerical approach is possible, and it is not difficult to find versions in almost any computational language or spreadsheet-. The graphical approach allows the visualization of concepts like the pinch if we work under the minimum reflux, the effect of different feed states in the column performance or the effect of intermediate heat exchangers, etc.

For mixtures of more than two components the Ponchon-Savarit method is practically not used at all. The reasons could be that for mixtures of more than two components the pure graphical method is not directly applicable “by hand” calculation loosing the important intuitive characteristics of the original method. For mixtures of more than 3 components is not possible any graphical representation at all. And the extension of graphical concepts to systems of three or more dimensions is not completely intuitive. However the classical Ponchon-Savarit method presents some characteristics that made very attractive the extension to multicomponent systems: a) Robustness. The convergence for a feasible postulated separation is almost always guarantied. b) In each iteration a near optimal design is obtained. If for any reason the system does not converge any intermediate design is almost a feasible solution. c) The speed of convergence is similar to those in standard simulation packages. d) For mixtures of three components it is possible generate three dimensional images similar to those for binary mixtures with the corresponding insight about the process we are studying.

The extension of graphical methods for systems of more than two components, and especially for systems involving three components (very important for instance in azeotropic separation) could be a valuable help for complementing the actual design tools with a robust, intuitive, fast, easy to implement and in most cases with graphical information about the process. As examples, Lee et al.[3], Reyes et al.[4] and Marcilla et al.[5] have presented an extension of the

Ponchon-Savarit method to reactive distillation, minimum reflux ratio calculation and quaternary liquid-liquid extractors, respectively.

Additionally, the use of topological analysis has been applied with success in the design of unit operations[6,7], calculation of distillation boundaries[8], and in the simultaneous correlation of complex phase equilibria including condensed phases: LL[9-14], LS[15], LLS[16] and LLSh[17].

In the rest of paper we present an extension to multicomponent mixtures of the classical Ponchon-Savarit method, especial attention is paid to three components mixtures due to the physical insight gained by graphical representations. The use of different approximate approaches in order to avoid iterations in the equilibrium and mass balance calculations are also introduced. Results obtained are compared with conventional rigorous method, showing very good agreement.

2. Extension to multicomponent systems of the Ponchon and Savarit method

An extension of the Ponchon-Savarit method to solve the problem of the separation of a binary mixture in a complex column was proposed by Marcilla et al[18]. The extension of this procedure to multicomponent mixtures can be easily made if explicit functions for the saturated vapor enthalpy, saturated liquid enthalpy and saturated liquid composition of the type $H=H(y_i,T,P)$, $h=h(x_i,T,P)$ and $x_i=x(y_i,T,P)$ are available. In other case, conventional equilibrium calculations must be carried out, or approximate methods can be developed. In this work, the two approaches have been developed in the rigorous and approximate methods. The enthalpy functions have been generated from fittings of the equilibrium data in all the composition range to polynomial functions. These functions have also been combined with different suggested interpolation and correlation methods in order to obtain the equilibrium compositions at each stage.

Figure 1 shows a sketch of the location of the net flow points $\Delta_{\underline{k}}$ and the graphical solution of a simple column for a ternary system, as in the classical Ponchon-Savarit method for binary mixtures. Obviously, systems with more than three components cannot be graphically represented and the problem must be solved by the use of computational methods. Nevertheless, these methods are still based on the same geometrical concepts as those used for the binaries in combination with the algorithms that involve the corresponding equations

for the equilibrium conditions and mass and enthalpy balances for a general type of complex column. This column is divided into *k* sections, each one having a characteristic net flow rate (difference between the streams that cross each other between stages), the changes from one section to the following occur whenever a side stream (of mass or heat) is added or removed (see Figure 2). $\sum F_{k-1}$ represents all the feeds entering the column above the zone *k* of the column (with enthalpy H^F_{k-1} and composition $z^F_{i,k-1}$. $\sum P_{k-1}$ represents all the side products removed from the column above the zone k (with enthalpy H^P_{k-1} and composition $z^p_{i,k-1}$. The separation between each two adjacent sectors occurs at a feed point, at a side product point or at a heat addition or removal point.

To begin the problem of calculation of the number of trays as in the Ponchon-Savarit method, the coordinates of the net flow points representative of each sector, Δ_k, must be calculated and the equation of the operative lines (representative of the mass and enthalpy balances) must be obtained. To do this, the following equations are used:

Composition of the net flow point Δ_k

$$\delta_{i,k} = \frac{\sum_k P_{k-1}\ z^P_{i,k-1} + D\ x^D_i - \sum_k F_{k-1} \cdot z^F_{i,k-1}}{\sum_k P_{k-1} + D - \sum_k F_{k-1}} \qquad (1)$$

Enthalpy of the net flow point Δ_k

$$M_k = \frac{\sum_k P_{k-1}\ H^P_{k-1} + D\ h^D + Q^D + \sum_k Q^E_{k-1} - \sum_k Q^A_{k-1} - \sum_k F_{k-1} \cdot H^F_{k-1}}{\sum_k P_{k-1} + D - \sum_k F_{k-1}} \qquad (2)$$

Equation of the operative line (mass and enthalpy balance line) in the enthalpy-composition diagram, that relates the saturated vapor leaving stage *j* in the zone *k* with the saturated liquid leaving stage *j+1* in the same sector, and passing through the point representative of Δ_k (difference between these vapor and liquid streams).

$$\frac{L_{j+1,k}}{V_{j,k}} = \frac{y_{i,j,k} - \delta_{i,k}}{x_{i,j,k} - \delta_{i,k}} = \frac{H_{j,k} - M_k}{h_{j+1,k} - M_k} \qquad (3)$$

where i extends for the different components.

To find the analytical solution, two problems must be solved (Reyes et al.[19]): a) establish a procedure to calculate the vapor-liquid equilibrium and to obtain the liquid phase in equilibrium with a given vapor phase (or vice versa) in each tray in a rigorous or approximate way, and b) to set up a procedure to obtain the intersection point between the operative line and the enthalpy-composition surface (in the enthalpy/composition n-dimensional space), also in a rigorous or approximate way.

2.1. Procedures to calculate the vapor-liquid equilibrium

The methods developed in this work fall into two categories:

a) the rigorous method, where the equilibrium data have been obtained using a given equation of state or activity model. We have used the NRTL model. This method obviously involves an iterative calculation method wherever an equilibrium composition is required.

b) the approximate methods that allow the determination of the composition in equilibrium with any given phase in equilibrium and without any iterative calculation, using:

b.1) On one hand, *interpolation methods* on two lattices of equilibrium points in all the composition range, generated previously by the rigorous procedure (a regular ordered lattice with the points representative of the saturated vapor, as well as the lattice for the points of the corresponding saturated liquids, see Figure 3). The interpolation procedures proposed are the following:

- Simple interpolation with distances
- Interpolation by intercepting lines from the three, four or twelve nearest points.
- Interpolation from linear fitting of compositions or compositions and enthalpies.

In Appendix A we describe the interpolation by intercepting parabolic lines from the twelve points proposed, the other interpolations proposed can be found in Marcilla et al.[20].

b.2) On the other hand, an *empirical correlation* of equilibrium data are suggested to calculate directly the liquid-vapor equilibrium in an approximate way. The equation proposed for the liquid-vapor equilibrium data correlation is the following (although any other empirical equation could be used[21]), and the complete development of this procedure is described in Appendix B:

$$\log\left(\frac{\lambda_j}{\lambda_i}\right) = \mathrm{A} + \mathrm{B}\cdot\log\left(\frac{\eta_j}{\eta_i}\right) + \Phi\cdot\left(\log\left(\frac{\eta_j}{\eta_i}\right)\right)^2 \qquad (4)$$

This procedure was previously adopted for the rigorous design of multistage extraction[5,22].

All these approximate procedures to calculate the liquid-vapor equilibrium (interpolation and correlation) have the advantage that, despite requiring the previous generation of the equilibrium nets, they do not require iterative calculations thus saving calculation time.

2.2. Procedures to calculate the mass and energy balances

In the Ponchon-Savarit method, the mass and energy balances connect two consecutive trays (streams crossing between plates) through the net flow, Δ_k, it means that the intersection between the operative line shown in Eqn. (3), that connects points Δ_k and $L_{j,k}$, with the surface defined by the points representing the saturated vapor, locate the next vapor $V_{j+1,k}$, see Figure 1. The procedures proposed in this work to solve this intersection are again of two types: i.e., approximate and rigorous methods. The approximate procedures requires a fitting of the equilibrium points in each phase to the corresponding enthalpy-composition polynomial functions (Eqn. 15) and its intersection with the operative lines (Eqn. 3) allows the mass and energy balances to be solved using a simple method, solving the corresponding system of equations. This method involves very short calculation times and yields very good results. The rigorous method to calculate the mass and energy balances is based on an iterative process that calculates the intersection between the rigorous enthalpy/composition function Eqn. (18) and the operative lines Eqn. (3). These procedures are described in Appendix C and D, respectively.

3. Description of the proposed procedure for the design of a rectification column

In the problem of designing a distillation column, only the percentage of recuperation of the heavy and light key components in the distillate and the residue are specified. In this case, it must be taken into account that, as opposed to the case of binary mixtures, for a multicomponent mixture a specification of this type does not permit calculation of the composition of the distillate, and the stage by stage calculation cannot be started unless initial estimates are made for the required variables to completely characterize the distillate (depending on the number of components).

For a ternary system only one variable must be assumed to fully determine the distillate composition and permit the calculation using the specification of the separation between key

components in combination with the material balances and the assumed variable. We have selected the distillate flow rate (D) as the variable to be optimized to allow the convergence between the bottom composition calculated by the overall mass balance (corresponding to the assumed distillate flow rate) and the bottom composition calculated (with successive tray by tray calculations) as that corresponding to the last tray leaving the column. In order to obtain an integer number of trays another variable should be simultaneously optimized. For this case we have selected first optimizing D and afterwards varying L_D in order to obtain the integer number of trays closer to that obtained in the previous step.

To determine the possible range of values of distillate flow D it is necessary to follow different steps:
The material balance for the column permits a range of pairs of values of distillate (D) and residue (R) flow rates (and their corresponding compositions) that satisfy the separation of the key components desired. Figure 4a shows the position of the two straight lines that represent the geometrical location of all possible values of $D\,x_1^D$ and $R\,x_3^R$ for a ternary system and for a distillation column with a single feed. All these points satisfy the material balances in the column, but only one, the one searched, is compatible with the equilibrium tray-by-tray calculations. Component 1 has been selected as the light key, and component 3 as the heavy key. Straight lines from a point on the line $D\,x_1^D =$ constant, to the line $R\,x_3^R$ = constant, represent all the possible mass balances in the column (streams D, F and R must be on a straight line), and the $\alpha\beta$ and $\alpha^I\beta^I$ lines define the extreme pairs of values of D and R.

Figure 5 shows a distillation path defined by the points representative of the liquids leaving each tray. When a distillate composition is established, the trajectory of the distillation marked by the equilibrium between the phases in each stage (and by the efficiency of trays) is fixed, as well as the location of the difference points or net flow points. As can be seen, not all the trajectories corresponding to any hypothetical distillation curve end at the point predicted by the material balances.

The optimum D flow rate will be the one that minimizes the distance between the point representative of the residue (as obtained by the mass balance) and the liquid composition exiting from the last calculated tray. In Figure 5, R_{1cal} represents a bottom product from a column and R_{1bal} the residue obtained from an overall mass balance. R_{2cal} and R_{2bal} are the

corresponding points of another hypothetical column, with a different distillate composition, but the same recovery of the key components. The D optimum has been calculated by minimization of the objective function defined by Eqn. 5:

$$d\left(x_i - x_i^R\right) = \sqrt{\sum_i \left(x_i - x_i^R\right)^2} \qquad (5)$$

where x(i) is the composition of the liquid phase from the last calculated stage (bottom product) and $x_R(i)$ is the composition of the bottom product obtained from the overall mass balance.

Therefore, the design procedure suggested involves the following steps:

Step 1. Starting point: specification of the variables:

- Characteristics of side streams (feeds, side products or heat additions or removals): flow rate, composition, enthalpy (thermal state) and code indicating a mass stream or a heat stream. The sign of flow indicates a feed or a side product.
- Pressure in the condenser and in the first tray of the column, and pressure drop by stage.
- Recovery percentage of the light key component (LK) in the distillate and of the heavy key (HK) in the residue.
- If it is the case, Reflux ratio (L_D/D).
- Thermodynamic data for the components of the system (rigorous method) or the lattice of equilibrium points and the coefficients of their fittings to polynomial functions (approximate methods).

Step 2. Determination of the range of variation for the distillate flow rate

Step 3. Select a starting D in the range determined (variable to be optimized).

Step 4. Calculation of the column. Once a distillate composition has been established, a bottom stream composition can be calculated by the mass balances, and the step by step calculation initiated, using the flowsheet showed in Figure 6.

The tray by tray calculation procedure starts at the top of column, from the distillate composition, which is the same as that of the vapor from the first tray, and calculating the liquid in equilibrium with this vapor. To pass to the next tray, it is necessary to solve the mass and energy balances. This can be done by connecting the point representative of the liquid

with the point representative of the net flow of the corresponding sector of the column Δ_k (operative line, Eqn. 3) and calculating the intersection of this straight line with the equilibrium surface corresponding to the saturated vapor: the intersection point is the vapor leaving the next tray. This procedure is repeated until the tray where a side stream k (feed or product in its optimum location) is reached, and where the change of sector (and of course of net flow point, Δ_{k+1}) is required.

The following criterion was used to test if the condition for the change of sector was reached: the last tray (*j*) in sector *k* is that verifying Eqn. (6):

$$\frac{x_{1,j,k} / x_{3,j,k}}{x_{C1,k} / x_{C3,k}} \leq 1 \qquad (6)$$

where x_C refers to the liquid in equilibrium at the point of intersection between the straight line that connects Δ_k and V_k^F (saturated vapor in equilibrium with the side stream F_k that separate sector k from sector k+1) and the saturated liquid surface (Figure 7). 1 and 3 are the indexes for light and heavy key components, respectively. The procedure continues, using the same criterion, until the residue composition calculated from the overall mass balance is reached or exceeded.

If the bottom composition as obtained by material balances is obtained for a stream leaving a given stage, the calculation is finished and the number of stages obtained is the solution of the design problem. Otherwise, the calculation must be repeated and another distillate composition must be selected until total convergence of the end of the distillation trajectory (equilibrium stream leaving the last calculated tray) and the bottom composition by overall mass balance.

When the side stream F_k is not a saturated vapor or liquid it is necessary to use in the change tray (and only in this tray) the net flow point Δc_k corresponding to F_k, see Figure 7. Δc_k is the intersection point between the straight line that connects Δ_k and V_k^F, and the other straight line that connects Δ_{k+1} and L_k^F. V_k^F and L_k^F are the liquid and vapor phases in equilibrium with the side stream F_k at the column conditions. This equilibrium phases can be obtained by whatever distillation flash procedure or by a iterative procedure using any of the

previous procedures proposed to calculate the vapor-liquid equilibrium, in order to find the corresponding tie line: $V_k^F - F_k - L_k^F$.

Figure 8 shows the general flowsheet of the design procedure suggested. We have developed three categories of calculation programs to design rectification columns: *rigorous program*, that rigorously solve the mass and energy balances and the equilibrium equations, *semi-rigorous programs,* that rigorously solve the equilibrium equations but only approximately the enthalpy balances and *approximate programs,* that approximately solve both enthalpy balances and equilibrium equations.

4. Examples

In order to test the validity of the proposed methods, computer programs were prepared, according to the previous procedures, and the design of 36 different simple distillation columns has been performed, varying the thermal condition of the feed and its composition, the nature of the equilibrium (ideal or nonideal), and using equilibrium surfaces with different density of points. The methods suggested have been applied to three different ternary mixtures:

a) benzene(1)-ciclohexane(2)-toluene(3)
b) methanol(1)- acetone(2)-water(3)
c) methanol(1)- ethyl acetate(2)- water(3)

The distillation columns analyzed are simple, with only one liquid feed, and with a total condenser that produces the distillate (D) and the reflux (L_D) streams at the bubble point, Table 1 shows the characteristics of each problem considered. The methods have been compared with the results obtained, for the same cases, by using the simulation program proposed by Renon et al[26]. An excellent agreement has been obtained in all cases and the results obtained for the design of the columns are showed in Table 2. In all cases the distances between the last calculated tray and the composition of the residue (from an overall mass balance) are very low. Several equilibrium lattices have been calculated for the systems, at varying composition increments (nets of 66, 231, 861 and 5151 equilibrium points -which correspond to mole fractions increments of 0.1, 0.05, 0.025 and 0.001, respectively- have been considered). These lattices have been used to test the influence of the composition

increment in the lattice (the number of equilibrium points in the lattice) on the accuracy of the different interpolation methods, as well as on the intersection of the operating lines with vapor surface.

As an example, Figure 9 compare the results obtained (composition profiles obtained for the component 1 along the column) from the rigorous design method presented in this work and the results from the Renon et al.[26] simulation method for cases 1 and 2. As can be seen, the results are exactly the same, as expected since both are rigorous methods. It should be noted that the proposed procedure presents several advantages over other methods found in literature, such as the short calculation time required and its theoretical simplicity as it is based on the same geometrical concepts as the Ponchon and Savarit method.

For the next discussion, the results obtained by the rigorous method proposed are used to test the validity of approximate and semi-rigorous methods. As an example, Figure 10a-b. shows the comparison between the results obtained for cases 1 and 3 by the approximate method, using a network with 66 points and the interpolation by intercepting lines from the twelve nearest points (to solve the equilibrium eqns.) and the intersection procedure with linear fitting of enthalpies (to solve the mass and energy balances) and the results obtained by the rigorous method. As can be seen in the figure, the interpolation procedure allows very coincident results. The results obtained for all the cases analyzed lead to similar conclusions.

To determine the effect of the density of points of the equilibrium net in the accuracy of the interpolation, Figure 10b-c shows the comparison between the results obtained for column 3 by the approximate methods, using again the interpolation by intercepting lines from the twelve nearest points and lattices with different number of points (increment in composition in mole fraction of 0.1, and 0.025, corresponding to lattices with 66 and 861 points, respectively). As can be observed, the agreement is excellent even for the less dense net. Similar results are obtained for the rest of components in both phases. Nevertheless, and as expected, it has been proved that the agreement increases as the density of points increases, and is always better for ideal systems than for nonideal systems. The distortion of the surfaces introduced by the equilibrium logically results in a loss of accuracy of the equations used to describe these surfaces. Nevertheless, the results could be improved by actualizing such equations to the different zones. This is an important conclusion because it allows a

multicomponent complex distillation column to be calculated in short time, as with shortcut methods, but with an accuracy close to that provided by rigorous methods.

Figure 11 shows results for column 1 and 2, respectively, when comparing the approximate method using the proposed correlation (Eqn. 4) to calculate the liquid-vapor equilibrium and intersection with fitting of enthalpies (Eqns. 15 to 17) and the rigorous method. The method in this case again yields excellent results.

The results obtained by the application of semirigorous methods to the examples obviously show the same influence of the spacing of the network: accuracy is greater when the number of points increases.

5. Conclusions

A direct design method has been suggested and applied to various cases of ternary mixtures with very satisfactory results. These procedures range from the approximate methods to a rigorous method, and are based on very simple geometrical concepts. The method has the following characteristics:

1. It is a design method very robust. The convergence, if the postulated separation is feasible, is almost always guarantied.
2. The method has the same conceptual simplicity as the Ponchon-Savarit method, and consequently it is very easily understood and intuitive.
3. At each iteration, a near optimal design is obtained with their distillate and residue flows and composition, optimum feed stage location as well as the number of stages for the specified separation.
4. With the approximate procedures, the iterations inherent to solve the equilibrium are eliminated by substitution by different types of interpolation or correlation between the points of the equilibrium surfaces. On the other hand, the resolution of the mass and energy balances is very simple by the calculation of the intersection between an operative line and a solubility surface (in the space of c dimensions, where c is the number of components).

Acknowledgements

Support from University of Alicante (under the project GRE01-03) and Institute of Culture Juan Gil Albert (County Council of Alicante, Spain) are gratefully acknowledged.

List of symbols

A, B, C, D, E	coefficients of a fitting of the equilibrium surfaces
a(m), b(m), c(m)	coefficients of quadratic fitting in the interpolation method
a_i, b_i, c_i, d_i, e_i, f_i	equilibrium correlation parameters of the model proposed
C	constant used in the variable change that permits to include in the correlation the binary and ternary equilibrium data
Component 1	light key component
Component 3	heavy key component
D	distillate flow or point representative of the distillate in the diagrams
D(1), D(2)	possible distillates according to the separation specified
D(m, n)	distance between P(m, n) and P_o
D'(m, n)	distance between P'(m, n) and P_o'
$D(x_i - x_i^R)$	euclidean distance
F	feed flow or point representative of the feed in the diagrams
H	enthalpy of a vapour stream
$H_{j,k}$	enthalpy of a vapour stream leaving tray j in sector k
H^D	enthalpy of the vapour leaving the top of the column
H	enthalpy of a liquid stream
$h_{j+1,k}$	enthalpy of a liquid stream leaving tray j+1 in sector k
h^D	enthalpy of the distillate (liquid)
H^F_{k-1}	enthalpy of the feed between sectors k-1 and k
H^P_{k-1}	enthalpy of the side product between sectors k-1 and k
HK	heavy key component
i.	index referring to a component
j.	index referring to a tray
k.	index for a sector of a distillation tower
K_i	equilibrium constant for component *i*
L_D	reflux flow
L^F_k	saturated vapour in equilibrium with the feed F_k
$L_{j+1,\,k}$	liquid stream leaving a tray j + 1 in the sector k
LK	light key component
Lv	liquid-vapour mixture
M_k	enthalpy of the net flow point
M, n	index referring to relative positions of the nearest points for the interpolation method
Ov	overheated vapour
P(m, n)	point on the surface of the saturated liquid, nearest to P_o, with

	composition $y_{i,j,k}$,(m, n)
P_o	point representative of the saturated liquid whose vapour in equilibrium must be obtained, with composition $y_{i, j, k}$
P_o'	point representative of the saturated vapour in equilibrium with P_o, with composition $x_{i, j, k}$
P'(m, n)	representative points of the saturated vapour in equilibrium with p(m, n), with composition $x_{i, j, k}$(m, n)
Q^D	heat duty in the condenser
R	residue flow or point representative of the residue in the diagrams
R_{1bal}, R_{2bal}	possible residue points obtained from an overall mass balance
R_{1cal}, R_{2cal}	possible residue points obtained from a tray-to-tray calculation (liquid streams from the last tray)
r.	index referring to equilibrium surface (saturated vapour or liquid)
sl	saturated liquid
sv	saturated vapour
ul	undercooled liquid
V^F_{k-1}	saturated vapour in equilibrium with the feed F_{k-1}
$V_{j, k}$:	vapour stream leaving a tray j in the sector k
x_i	composition of component i in a liquid stream
$x_{i, j, k}$	composition of component i in the liquid stream leaving stage j of sector k
$x_{i,j,k}$(m, n)	composition of liquid P'(m,n). The indexes i, j, k are those corresponding to the point P_o
$x^C_{i, k}$	composition of component i in the saturated liquid in the intersection between saturated liquid surface and the straight-line Δ_k-Δ_C
x^D_i	composition of component i in the distillate
x^F_i	composition in component i in the saturated liquid in equilibrium with the feed
x^R_i	composition of constituent i in the residue
y_i	composition of component i in a vapour stream
$y_{i, j, k}$	composition of component i in the vapour stream leaving stage j of sector k
$y_{i,j,k}$(m, n)	composition of vapour P(m,n). The indexes i, j, k are those corresponding to the point P_o
z^F_{k-1}	composition of the feed between sectors k-1 and k
z^P_{k-1}	composition of the side product between sectors k-1 and k
ΣF_{k-1}	sum of all feeds entering above sector k in a complex column
ΣP_{k-1}	sum of all products leaving the column above sector k
ΣQ^E_{k-1}	sum of all heat removed above sector k in a complex column

ΣQ^{F}_{k-1}	sum of all heat inputs above sector k in a complex column

Greek characters

A, B, Φ and α, β, ϕ	Parameters of the logarithmic equation used to correlate the liquid-vapour and the liquid-liquid equilibrium data, respectively
α, α', β, β'	limits for the possible $R \cdot x^{R}(3)$ and $D \cdot x^{D}(1)$ values
Δ_k	net flow point corresponding to the sector k
Δ_C	net flow point corresponding to the feed zone
$\delta_{i,k}$	composition of the net flow point of sector k
$\lambda(i), \lambda(j), \lambda(k), \lambda(l)$:	Normalised coordinates of the searched phase (vapour phase in the L-V equilibrium and organic phase in L-L equilibrium)
$\eta(i), \eta(j), \eta(k), \eta(l)$:	Normalised coordinates of the known phase (liquid phase in the L-V equilibrium and aqueous phase in L-L equilibrium)

References

[1] Sorel, E. *La rectification de l'alcohol*; Gautier-Villais et fills: Paris, **1893**.

[2] Ponchon, M. Graphical study of distillation. *Tech. Modern.* **1921**, 13, 20.

[3] Lee, J.W., S. Hauan, K.M. Lien, and A.W. Westerberg, A Graphical Method for Designing Reactive Distillation Columns: I. the Ponchon-Savarit Method, *Proc. of the Royal Society A: Mathematical, Physical & Engineering Sciences*, **2000** Vol. 456(2000), 1953 –1964.

[4] J.A. Reyes, A. Gómez and A. Marcilla. Graphical concepts to orient the Minimum Reflux Ratio Calculation on Ternary Mixtures Distillation. *Ind. Eng. Chem. Res.* **2000**. 39, 3912-3919.

[5] Marcilla, A.; Gómez, A.; Reyes, J.A.; Olaya, M.M. New method for quaternary systems liquid-liquid extraction tray to tray design. *Ind. Eng. Chem. Res.* **1990**; 38(8): 3083-3095.

[6] Gómez A., Ruiz F., Marcilla A., Reyes J., Menargues S. Diseño de la separación de mezclas ternarias (I). Conceptos gráficos del equilibrio entre fases. *Ingeniería Química* 2001; 377: 219-229.

[7] Gómez A., Ruiz F., Marcilla A., Reyes J., Menargues S. Diseño de la separación de mezclas ternarias (II). Aplicación de conceptos gráficos a la separación de mezclas azeotrópicas. *Ingeniería Química* 2001; 379: 253-262.

[8] Reyes-Labarta, J.A., Caballero, J.A., Marcilla, A. Numerical Determination of Distillation Boundaries for Multicomponent Homogeneous and Heterogeneous Azeotropic Systems. Computer Aided Chemical Engineering 2010; 28: 643-648 (European Symposium of Computer Aided Process Engineering-20).

[9] Marcilla, A.; Olaya, M.M.; Serrano, M.D.; Reyes-Labarta, J.A. Methods for improving models for condensed phase equilibrium calculations. *Fluid Phase Equilib.* 2010; 296(1): 15-24.

[10] Marcilla, A; Olaya, M.; Serrano M.D.; Reyes-Labarta, J.A. Aspects to be considered for the development of a correlation algorithm for condensed phase equilibrium data for ternary systems. Ind. Eng. Chem. Res. 2010; in press.

[11] Reyes-Labarta J.A, Olaya M., Velasco R., Serrano M.D., Marcilla A. Correlation of the liquid-liquid equilibrium data for specific ternary systems with one or two partially miscible binary subsystems. *Fluid Phase Equilib.* 2009; 278: 9-14.

[12] Marcilla, A.; Olaya, M.M.; Serrano, M.D.; Velasco, R.; Reyes-Labarta J.A. Gibbs energy based procedure for the correlation of type 3 Ternary systems including a three liquid phases region. *Fluid Phase Equilib.* 2009; 281(1): 87-95.

[13] Olaya, M.M.; Reyes-Labarta, J.A.; Velasco, R.; Ibarra, I.; Marcilla, A. Modelling liquid-liquid equilibria for island type ternary systems. *Fluid Phase Equilib.* 2008; 265: 184-191.

[14] Olaya, M.M; Ibarra, I.; Reyes-Labarta, JA.; Serrano, M.D.; Marcilla, A. Computing liquid-liquid phase equilibria: an exercise for understanding the nature of false solutions and how to avid them. *Chem. Eng. Educ.* 2007; 41(3): 218-224.

[15] Reyes, J.A.; Conesa, J.A.; Marcilla, A.; Olaya, M.M. Solid-liquid equilibrium thermodinamics: checking stability in multiphase systems using Gibbs Energy Function. *Ind. Eng. Chem. Res.* 2001; 40: 902-907.

[16] Olaya, M.M.; Marcilla, A.; Serrano, M.D.; Botella, A.; Reyes-Labarta, J.A. Simultaneous correlation of liquid−liquid, liquid−solid, and liquid−liquid−solid equilibrium data for water + organic Solvent + salt ternary systems. Anhydrous solid phase. *Ind. Eng. Chem. Res.* 2007; 46: 7030-7037.

[17] Marcilla, A.; Reyes-Labarta, J.A.; Olaya, M.M.; Serrano M.D. Simultaneous correlation of liquid-liquid, liquid-solid, and liquid-liquid-solid equilibrium data for water + organic solvent + salt ternary systems: hydrated solid phase formation. *Ind. Eng. Chem. Res.* 2008; 47: 2100-2108.

[18] Marcilla, A, Ruiz, F. and Gómez, A. Graphically found trays and minimum reflux for complex binary distillation for real Systems. *Latin American Applied Research,* **1995,** 25, 87-96.

[19] Reyes Labarta, J.A.; Diseño de Columnas de Rectificación y Extracción Multicomponente. Cálculo del Reflujo Mínimo. Ph.D. Dissertation, University of Alicante, **1998** (http://www.cervantesvirtual.com/FichaObra.html?Ref=4845).

[20] Marcilla, A., Gómez, A. and Reyes, J.A. New Method for Designing Distillation Columns of Multicomponent Mixtures. *Latin American Applied Research,* **1997**, 27(1-2), 51-60.

[21] Marcilla A., Reyes-Labarta J.A., Velasco R., Serrano M.D., Olaya M.M. Explicit equation to calculate the liquid-vapour equilibrium for ternary azeotropic and non azetropic systems. VIII Iberoamerican Conference on Phase Equilibria and Fluid Properties for Process Design. EQUIFASE'09 Book of abstracts 2009b: 87 (http://hdl.handle.net/10045/14276).

[22] Reyes-Labarta, J.A. and Grossmann I.E.; Disjunctive optimisation Design Models for Complex Liquid-Liquid Multistage Extractors. **2001**. *AIChE J*. 47(10) 2243-2252.

[23] Foucher E.R.; Doherty M.F. and Malone M.F. Automatic Screening of Entrainers for Homogeneous Azeotropic Distillation. *Ind. Eng. Chem. Res.,* **1991**, 30, 760-772.

[24] Safrit B.T. and Westerberg A.W. Algorithm for Generating the Distillation Regions for Azeotropic Multicomponent Mixtures. *Ind. Eng. Chem. Res.,* **1997**, 36, 1827-1840.

[25] Stichlmair J.G. and Herguijuela J.R. Separation Regions and Processes of Zeotropic and Azeotropic Ternary Distillation. *AIChE J.***, 1992**, 38, 10, 1523-1535.

[26] Renon, H.; Asselineau, L.; Cohen, G. et Raimbault, C. Calcul sur ordinateur des équilibres liquide-vapeur et liquide-liquide. *Publications de l'Institut Français du Pétrole, Collection "Science et Technique du Pétrole.* **1971**, nº 17.

Appendix A. The approximate procedure proposed to calculate the vapour-liquid equilibrium using interpolations.

This procedure has the following steps:

a) Find the twelve nearest points, P(m, n) of composition $y_{i,j,k}(m, n)$, to the point P_o of composition $y_{i,j,k}$ to be interpolated (in the ordered lattice of saturated vapour). The index *m* refers to each one of the four series of points in Figure A1, the index n refers to each of the three points of the 4 series mentioned above. The three indexes (i, j, k) correspond to the co-ordinates of the point to be interpolated, i being related to the component, j to the tray and k to the sector. As can be seen in Figure A2 the twelve selected points can adopt different figures around the point to be interpolated, depending on the position of this point in the grid.

b) Determine the corresponding points in the conjugated net, P'(m, n) of composition $x_{i, j, k}$ (m, n), in equilibrium with the twelve P(m,n).

c) Set the origin of each series of points (i.e., the points: $x_{i, j, k}$ (m, 1) and $y_{i, j, k}$ (m, 1)) and calculate the distance of each point of each series to its corresponding origin:
Origin net:

$$d(m,n) = \sqrt{\sum_{i=1}^{3}\left(y_{i,j,k}(m,n) - y_{i,j,k}(m,1)\right)^2} \tag{7}$$

Destination net:

$$d'(m,n) = \sqrt{\sum_{i=1}^{3}\left(x_{i,j,k}(m,n) - x_{i,j,k}(m,1)\right)^2} \tag{8}$$

d) These distances to the respective origin are fitted for each one of the m series to parabolas of the type:

$$d'(m,n) = a(m)\cdot d(m,n)^2 + b(m)\cdot d(m,n) + c(m) \tag{9}$$

where a(m), b(m) and c(m) are the fitting coefficients: Thus for each sequence (m = 1, 2, 3, 4) a system of three equations (each equation corresponding to each one of the three points (n=1, 2, 3) of the series) with three unknowns that must be solved to obtain the coefficients of each parabola m (m = 1, 2, 3, 4):

$$\left.\begin{aligned} d'(m,1) &= a(m)\cdot d(m,1)^2 + b(m)\cdot d(m,1) + c(m) \\ d'(m,2) &= a(m)\cdot d(m,2)^2 + b(m)\cdot d(m,2) + c(m) \\ d'(m,3) &= a(m)\cdot d(m,3)^2 + b(m)\cdot d(m,3) + c(m) \end{aligned}\right\} \rightarrow a(m), b(m), c(m) \tag{10}$$

e) Once the coefficients of the 4 parabolas have been obtained, the points P(m,5) of the Figure 12 must be obtained: the point P(1,5) is calculated as the intersection between the lines passing through the points P(1,2) and P(1,3) and the line passing through P_o is parallel to the line passing through P(1,3) and P(2,3). The rest of the points are obtained in a similar way.

In order to calculate the corresponding compositions in equilibrium with these four points P(m,5), i.e., the four P'(m, 5) points, it is necessary:

- To calculate their corresponding distances, d'(m, 5), in the destination net using the parabolas and distances previously calculated in the origin net.

- Once the distances d'(m, 5) have been calculated, the points P'(m, 5) are located using the lever rule between the points P'(m, 1), P'(m, 5) and P'(m, n), for 1<m<4 and 2<n<4. Thus, for instance, in order to determine the coordinates of the point P'(1,5) the following equation is applied:

$$\frac{x_{i,j,k}(1,1) - x_{i,j,k}(1,5)}{x_{i,j,k}(1,1) - x_{i,j,k}(1,3)} = \frac{d'(1,5)}{d'(1,3)} \tag{11}$$

and:

$$x_{i,j,k}(1,5) = x_{i,j,k}(1,1) - \frac{d'(1,5)}{d'(1,3)} \cdot \left(x_{i,j,k}(1,1) - x_{i,j,k}(1,3)\right) \tag{12}$$

The coordinates of the rest of the points, P'(2,5), P'(3,5), P'(4,5), are obtained in a similar way. Finally, the point P'_o, which is the result sought for, is obtained as the intersection between the two straight lines P'(1,5)-P'(2,5) and P'(3,5)-P'(4,5), as shown in Figure A1. This method with twelve points provides very accurate results, even for nets with low density of equilibrium points.

Appendix B. The approximate procedure proposed to calculate the vapour-liquid equilibrium using empirical correlation.

The equation proposed for the liquid –vapour equilibrium data correlation is:

$$\log\left(\frac{\lambda(j)}{\lambda(i)}\right) = A + B\cdot\log\left(\frac{\eta(j)}{\eta(i)}\right) + \Phi\cdot\left(\log\left(\frac{\eta(j)}{\eta(i)}\right)\right)^2 \qquad (4)$$

with: $A = a_1 + b_1\cdot\eta(k) + c_1\cdot\eta(l) + d_1\cdot(\eta(k))^2 + e_1\cdot(\eta(l))^2$

$B = a_2 + b_2\cdot\eta(k) + c_2\cdot\eta(l) + d_2\cdot(\eta(k))^2 + e_2\cdot(\eta(l))^2$

$\Phi = a_3 + b_3\cdot\eta(k) + c_3\cdot\eta(l) + d_3\cdot(\eta(k))^2 + e_3\cdot(\eta(l))^2$

$\eta(i),\eta(j),\eta(k),\eta(l)$ are the normalised coordinates of a known initial equilibrium point (liquid phase):

$$\eta(1) = \frac{x(1)}{1+h} + C;\ \eta(2) = \frac{x(2)}{1+h} + C;\ \eta(3) = \frac{x(3)}{1+h} + C;\ \eta(4) = \frac{h}{1+h} + C \qquad (13)$$

C = Constant used in the variable change that permits to include in the correlation the binary and ternary equilibrium data.

$\lambda(i),\lambda(j),\lambda(k),\lambda(l)$ are the normalised coordinates of the equilibrium point searched (vapour phase):

$$\lambda(1) = \frac{y(1)}{1+H} + C;\ \lambda(2) = \frac{y(2)}{1+H} + C;\ \lambda(3) = \frac{y(3)}{1+H} + C;\ \lambda(4) = \frac{H}{1+H} + C \qquad (14)$$

a_i, b_i, c_i, d_i... are the correlation parameters which depend on the nature of the system and on temperature, but are independent on the composition.

Obviously, using only one equation as Eqn. (4) the composition of a phase from the known composition conjugated phase can not be calculated. Therefore, to obtain the composition and the enthalpy of a phase in equilibrium with given known phase, it is necessary to combine (n) equations of this type (different and complementary) for a system of n components. When the correlation parameters have been calculated, it is possible to calculate the composition of the conjugated phase in equilibrium with another phase of known composition considering that the parameters A, B and Φ are constant for each type of equation (4).

Appendix C. Approximate methods to calculate the mass and energy balances

The approximate procedures proposed in this work require a fitting of the equilibrium points in each phase to the corresponding enthalpy-composition polynomial functions, as shown in Eqn. (15):

$$a \cdot (z(1))^2 + b \cdot (z(2))^2 + c \cdot z(1) + d \cdot z(2) + e \cdot H = 1 \tag{15}$$

where z can be x or y and H can be h or H depending on the phase. This equation represents parabolic surfaces, and its intersection with the operative lines (Eqn. 3) allows the mass and energy balances to be solved using a simple method, solving the system of equations. This method involves very short calculation times and yields very good results.

The solution for the enthalpy of this intersection point is of the type shown in Eqn. (16):

$$A \cdot h^2 + B \cdot h + C = 0 \tag{16}$$

and there are two possible solutions, but only one with a physical sense. The correct solution is selected by comparison with the average value of equilibrium enthalpy.

Another procedure that allows better results than that previously described is to find the three nearest points from the intersection point and afterwards obtain a linear fitting of their enthalpies versus their compositions (Eqn. 17):

$$h = c_1 \cdot x(1) + c_2 \cdot x(2) + c_3 \cdot x(3) \tag{17}$$

The coefficients of this fitting, in combination with the composition of the intersection point previously calculated, allow the procurement of a new enthalpy value, that once substituted in the Eqn. (3) of the operative line, allows a better estimate. This composition can be considered as definitive, or used in Eqn. (17) in an iterative process to find the best value of the intersection. Generally, after two or three iterations, the values are very stable.

Appendix D. Rigorous method to calculate the mass and energy balances

This method is based on an iterative process that calculates, in a rigorous way, the intersection between the rigorous enthalpy/composition function Eqn. (18) and the operative lines Eqn. (3), by solving the corresponding system of equations.

$$h_i = f(K_i, x_i, y_i, T, P) \tag{18}$$

The system of equations must be solved by an iterative procedure. In this case the problem has been solved by the procedure shown in Figure D1: calculation begins at an equilibrium point P_1, near to intersection point; its enthalpy h_1 allows the calculation of (by Eqn. 3) the composition of a point P_2, with the same enthalpy as P_1, but not in the equilibrium surface. A rigorous calculation with the composition of P_2, allows P_3 to be obtained, on the equilibrium surface with the same composition but different enthalpy. This point is used for the next iteration. This process continues until the difference between the two consecutive values of enthalpy is less than a small quantity previously fixed.

This procedure is, obviously slower than the approximate methods, but yields the most accurate results.

Figure Captions:

Figure 1. Graphical representation of the Ponchon-Savarit method for a ternary mixture.

Figure 2. General complex distillation column.

Figure 3. Lattices of equilibrium points for the nonideal system methanol-ethyl acetate-water.

Figure 4. Determination of the possible distillate and bottom streams locations for a specified separation.

Figure 5. Different distillation paths depending on the distillate flow rate for a given percentage separation.

Figure 6. Flowsheet of proposed program for calculation of a rectification column.

Figure 7. Location of the net flow point $\Delta c(k)$

Figure 8. Flowsheet of the program to calculate a rectification column optimizing the distillate flow rate.

Figure 9. Comparison between the composition profiles obtained for component 1 in the liquid phase, by the rigorous design method proposed in present work (■) and by the Renon et al.[52] (Δ) simulation method, for cases 1 and 2.

Figure 10. Comparison between the rigorous design method (■) and the approximate method (Δ) using a network with 66 (a-b) and 861 (c) points and the interpolation by intercepting lines from the 12 nearest points and the intersection procedure proposed, for cases 1 (a) and 3 (b-c).

Figure 11. Results for column 1 and 2, comparing the approximate method (Δ) using the proposed correlation (Eqn. 14) and intersection with fitting of entalphies (Eqns. 15 to 17) and the rigorous method (■).

Figure A1. Possible location of the twelve nearest points to the point of interpolation (P_o).

Figure A2. Intercepting lines for interpolation with twelve points. Location of the interpolated point (P'_o).

Figure D1. Sketch of the iterative calculation to determine the intersection point between an operative line and the enthalpy-composition surface

Table Titles:

Table 1. Different cases used to illustrate the proposed procedures for the distillation column design method. All cases work with a reflux ratio=2 (lv: liquid-vapor mixture, ov: overheated vapour, sl: saturated liquid, sv: saturated vapor, ul: undercooled liquid).

Table 2. Results of the rigorous design method column design method. All cases work with a reflux ratio=2.

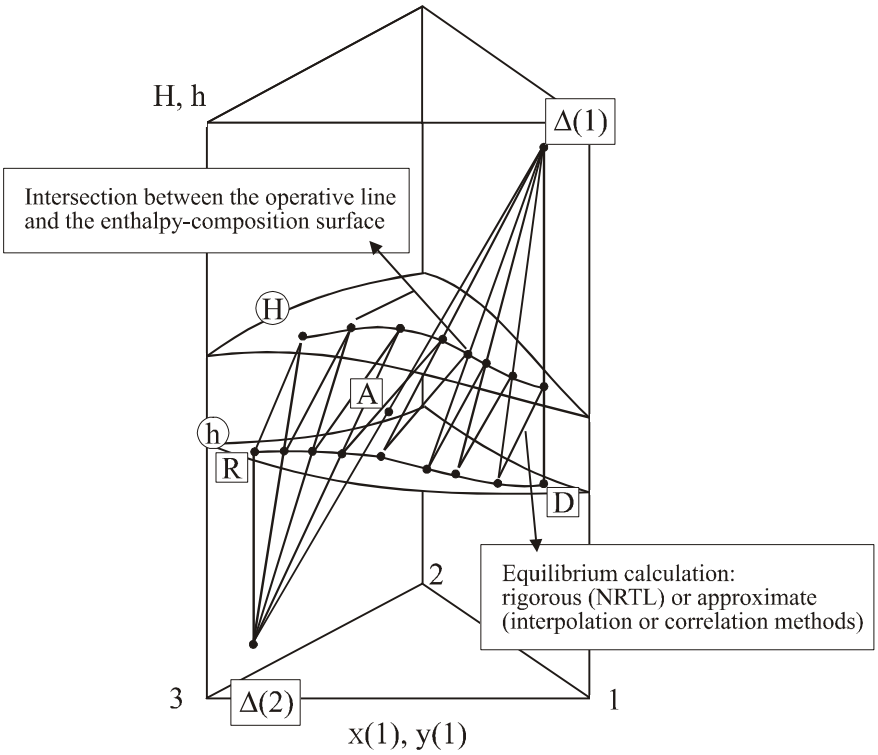

Figure1. Graphical representation of the Ponchon-Savarit method for a ternary mixture.

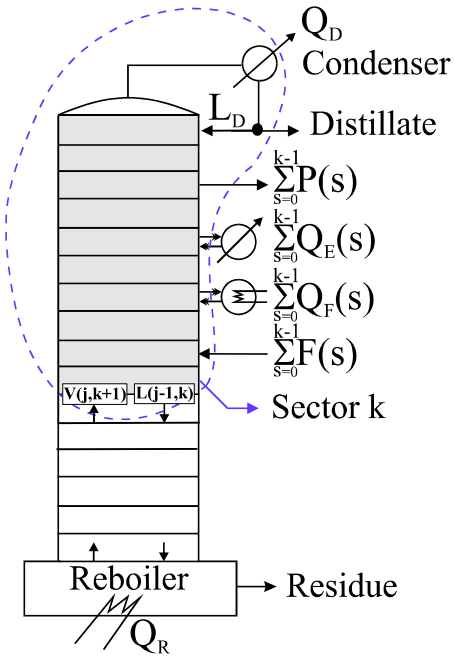

Figure 2. Generalized distillation column.

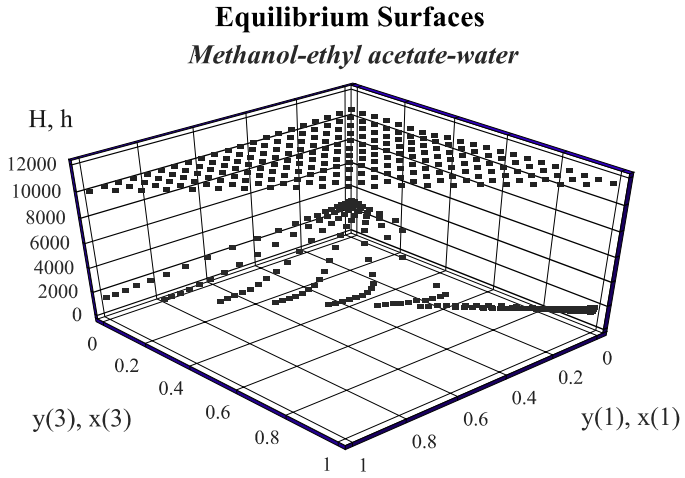

Figure 3. Lattices of equilibrium points for the non-ideal system methanol-ethyl acetate-water.

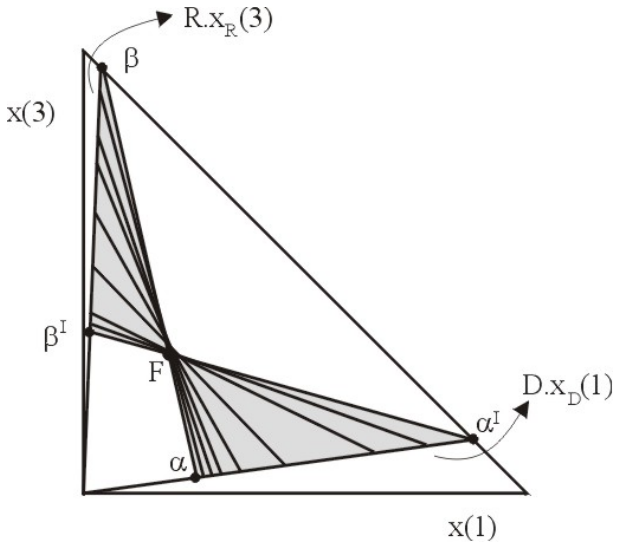

Figure 4. Determination of the possible distillate and bottom streams locations for a specified separation.

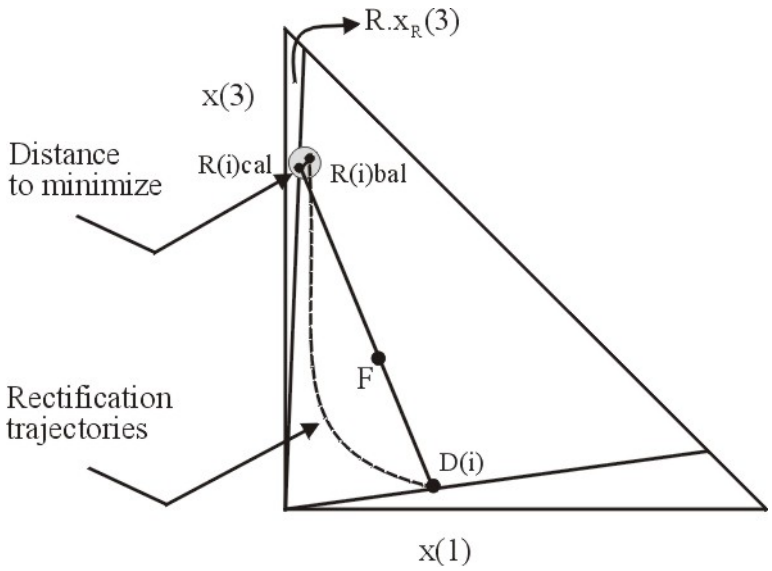

Figure 5. Distance to be minimized between the residue obtained with the overall mass balance and calculated as the last tray in the distillation column.

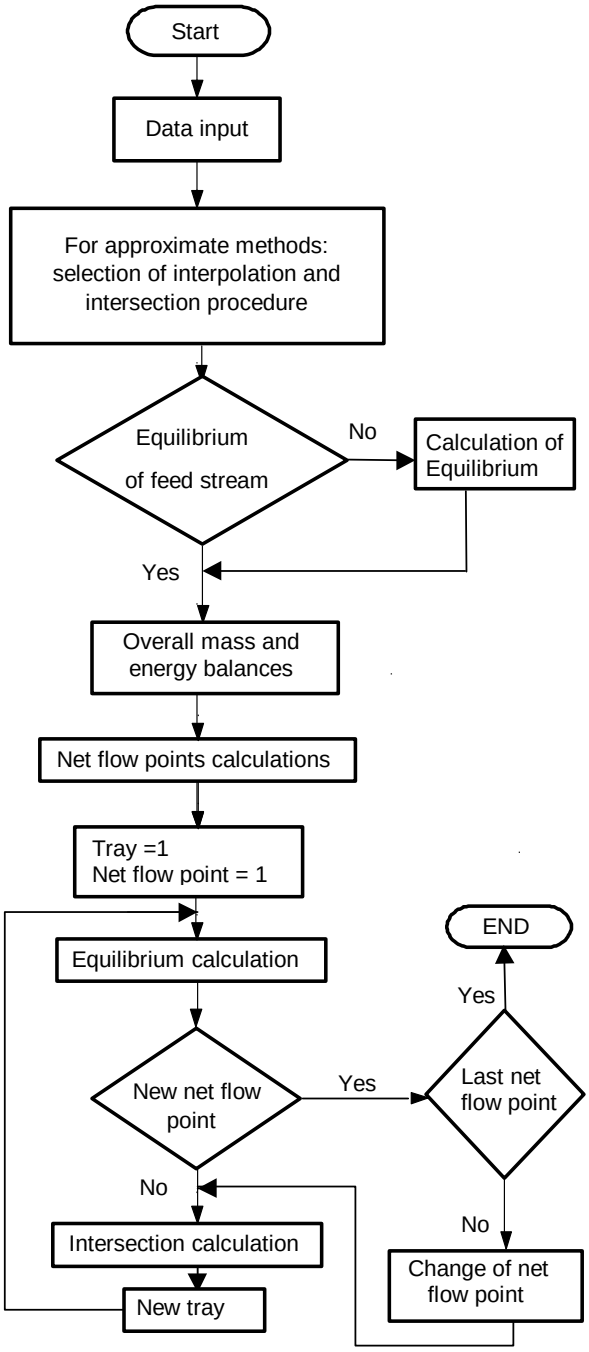

Figure 6. Flowsheet of the proposed program for calculation of a rectification column.

ISBN: 84-699-5991-3 (http://www.cervantesvirtual.com/FichaObra.html?Ref=4845)

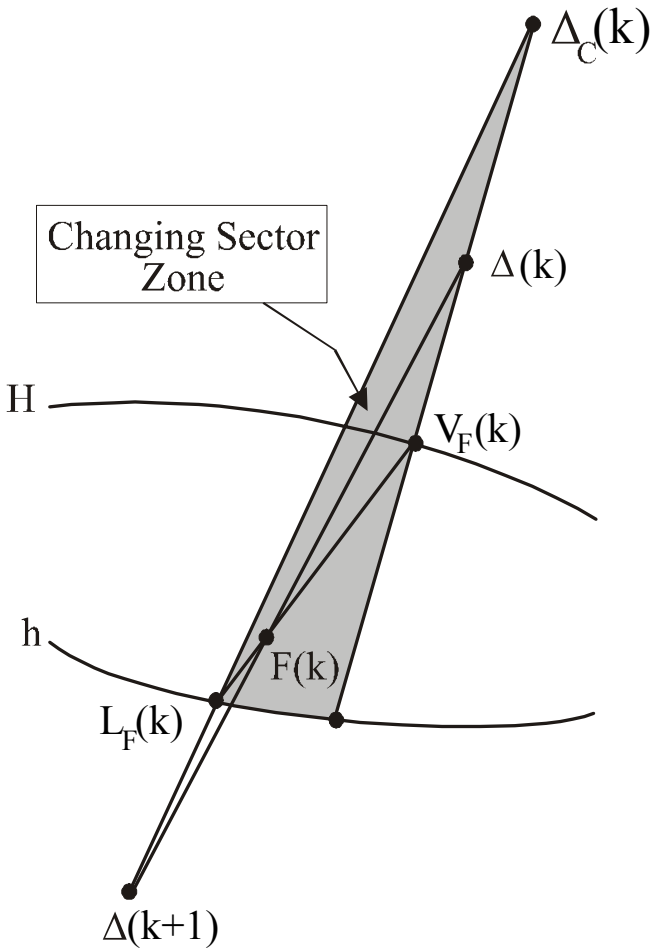

Figure 7. Location of the net flow point Δc(k)

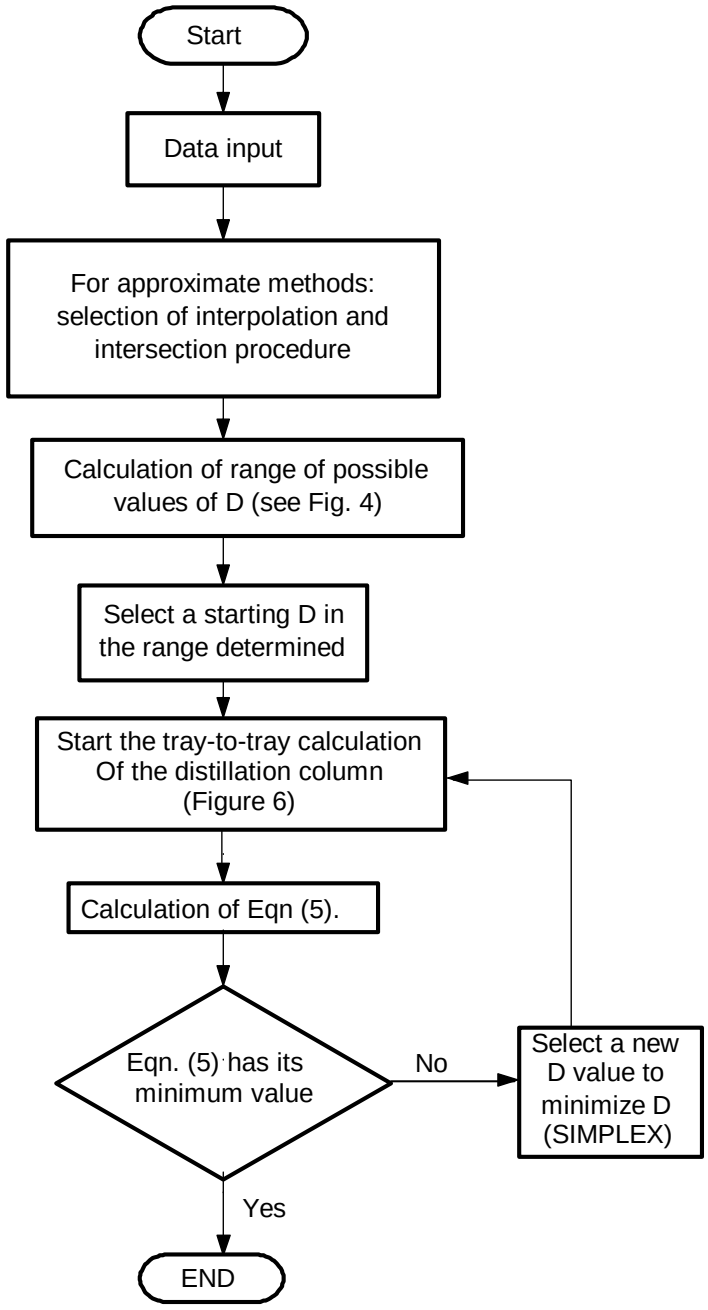

Figure 8. Flowsheet of the program to calculate a rectification column optimising the distillate flow rate.

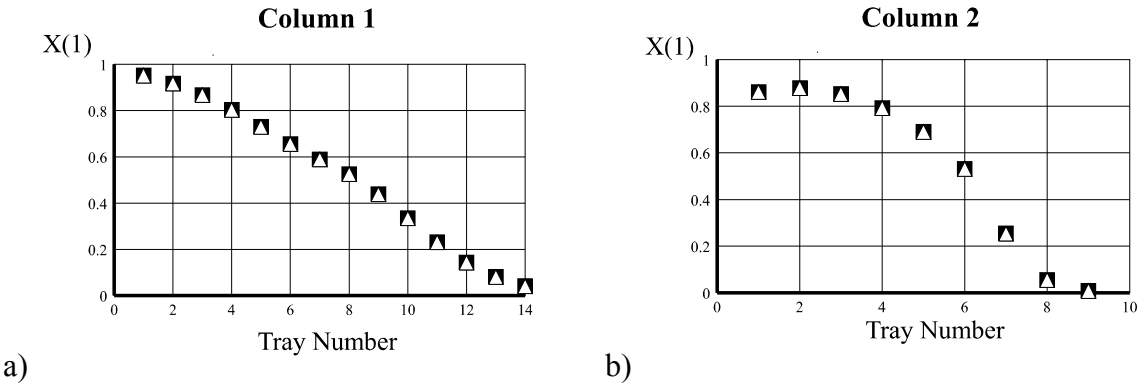

a) b)

Figure 9. Comparison between the composition profiles obtained for component 1 in the liquid phase, by the rigorous design method proposed in present work (■) and by the Renon et al.[13] simulation method (Δ), for cases 1 (a) and 2 (b).

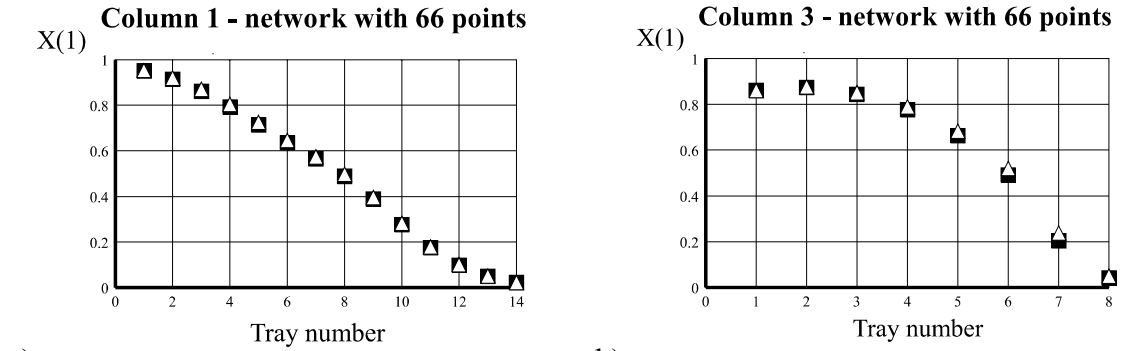

a) b)

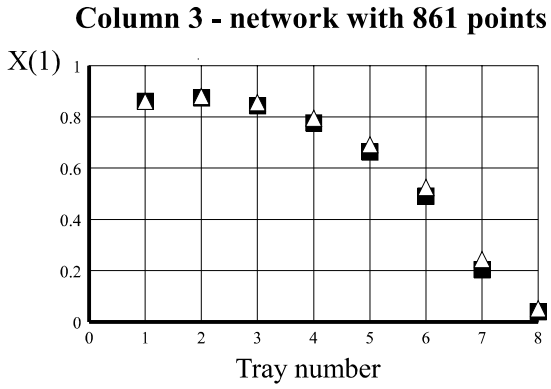

c)

Figure 10. Comparison between the rigorous design method (■) and the approximate method (Δ) using a network with 66 (a-b) and 861 (c) points and the interpolation by intercepting lines from the 12 nearest points and the intersection procedure proposed, for cases 1 (a) and 3 (b-c).

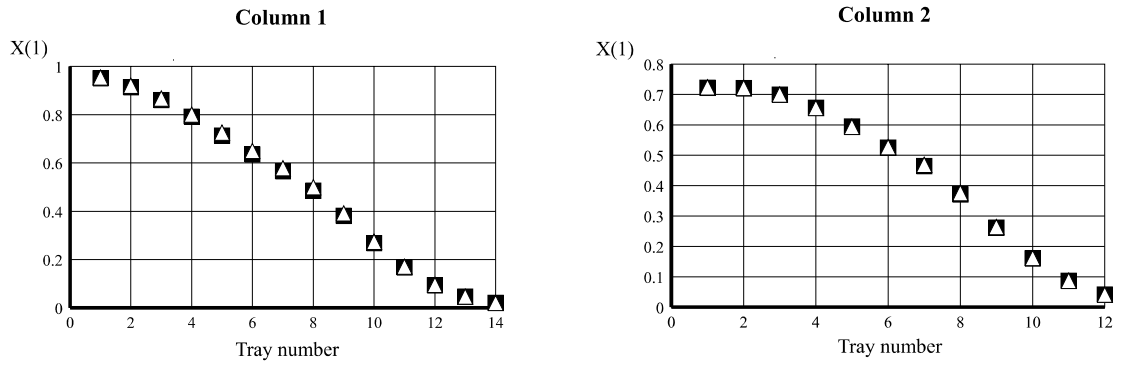

Figure 11. Results for column 1 and 2, comparing the approximate method (Δ) using the proposed correlation (Eqn. 14) and intersection with fitting of entalphies (Eqns. 15 to 17) and the rigorous method (■).

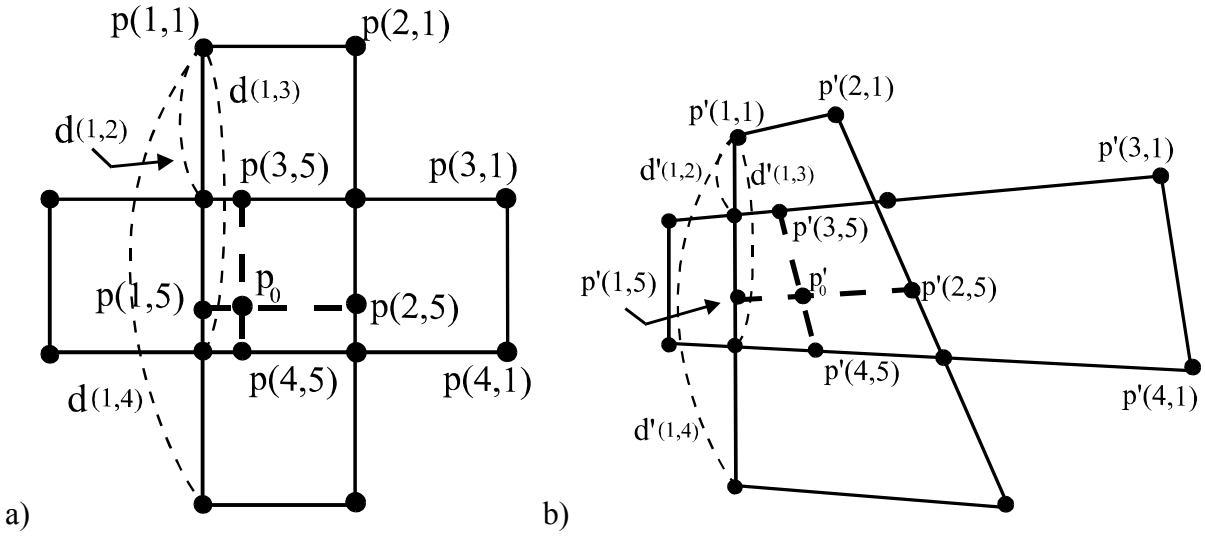

Figure A1. Possible location of the twelve nearest points to the point of interpolation (P_o).

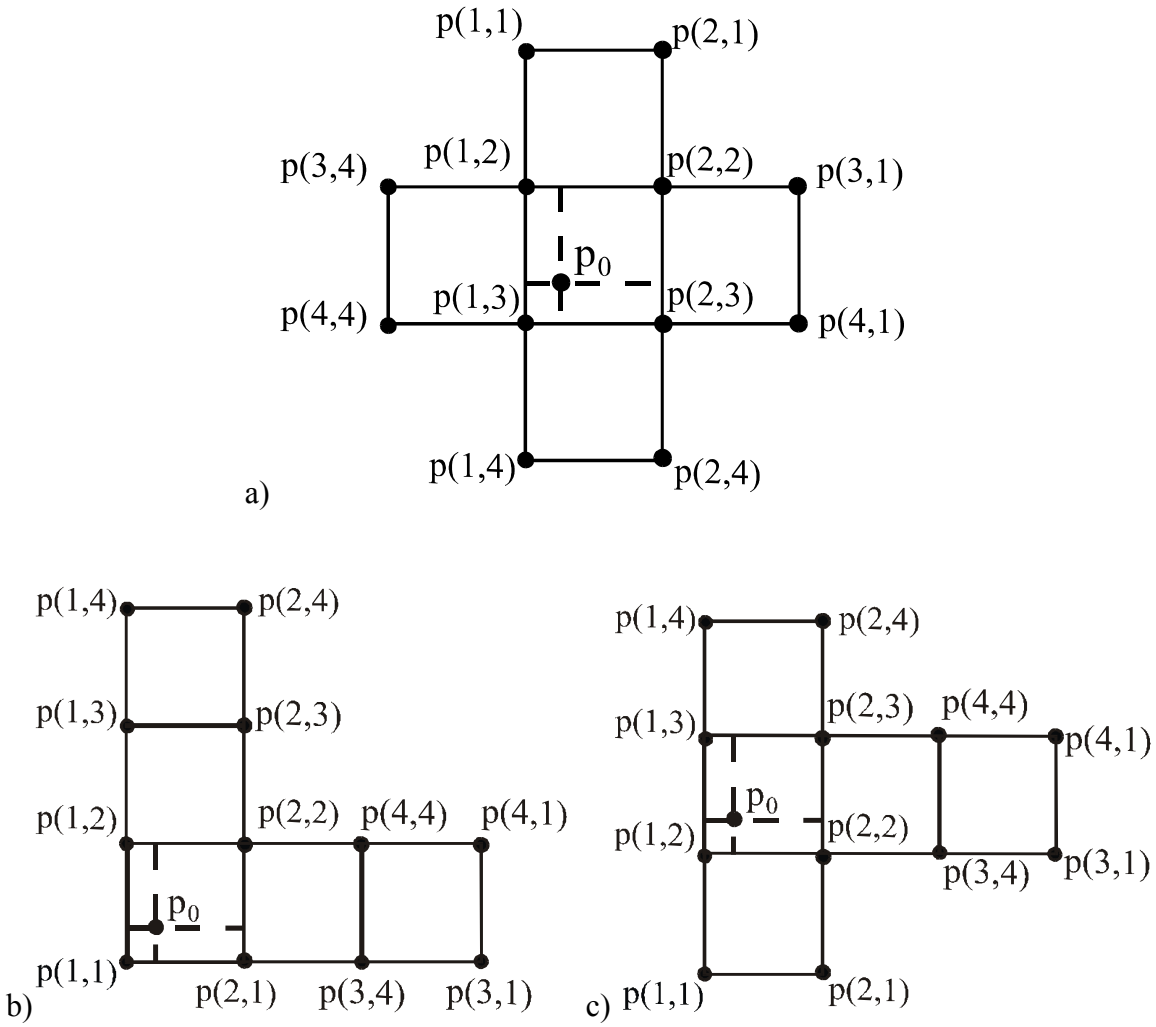

Figure A2. Intercepting lines for interpolation with twelve points. Location of the interpolated point (P'_o).

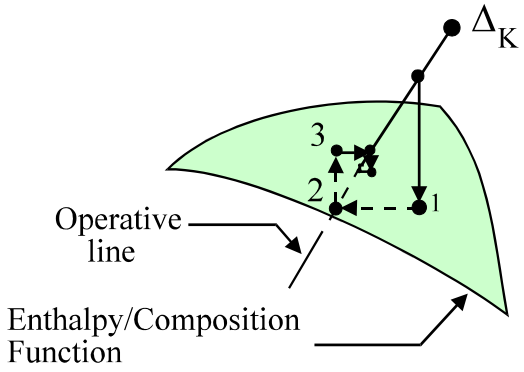

Figure D1. Sketch of the iterative calculation to determine the intersection point between an operative line and the enthalpy-composition surface

Table 1. *Different cases used to illustrate the proposed procedures for the distillation column design method. All cases work with a reflux ratio=2 (lv: liquid-vapor mixture, ov: overheated vapour, sl: saturated liquid, sv: saturated vapor, ul: undercooled liquid).*

Case	Mixture	Mole fraction of (1) ($z_F(1)$)	Mole fraction of (3) ($z_F(3)$)	Enthalpy h_F (kcal/mol)	Recovery percent (1)	Recovery percent (3)
1	a	0.60	0.394	3244 (sl)	97.3	97.4
2	a	0.50	0.30	3255 (sl)	97.4	98.2
3	a	0.18	0.50	3661 (sl)	97.3	97.4
4	a	0.70	0.12	2971 (sl)	97.3	97.4
5	a	0.30	0.30	3383 (sl)	97.3	97.4
6	a	0.394	0.60	3593 (sl)	90.0	90.0
7	a	0.10	0.30	3480 (sl)	97.3	97.4
8	a	0.50	0.40	3337 (sl)	97.3	97.4
9	a	0.40	0.40	3415 (sl)	97.3	97.4
10	a	0.40	0.40	3415 (sl)	90.0	90.0
11	a	0.50	0.30	3255 (sl)	97.0	97.0
12	b	0.55	0.30	1544 (sl)	96.9	97.6
13	b	0.30	0.50	1497 (sl)	97.0	94.0
14	b	0.25	0.35	1595 (sl)	96.9	97.6
15	b	0.55	0.15	1577 (sl)	96.9	97.6
16	a	0.60	0.394	2000 (ul)	97.3	97.4
17	a	0.60	0.394	7000 (lv)	97.3	97.4
18	a	0.60	0.394	11017 (sv)	97.3	97.4
19	a	0.60	0.394	12000 (ov)	97.3	97.4
20	a	0.50	0.30	2900 (ul)	97.4	98.2
21	a	0.50	0.30	7000 (lv)	97.4	98.2
22	a	0.50	0.30	10846 (sv)	97.4	98.2
23	a	0.50	0.30	12000 (ov)	97.4	98.2
24	b	0.55	0.30	1000 (ul)	97.4	98.2
25	b	0.55	0.30	7000 (lv)	97.4	98.2
26	b	0.55	0.30	10387 (sv)	97.4	98.2
27	b	0.55	0.30	11000 (ov)	97.4	98.2
28	b	0.40	0.40	1785 (sl)	90.0	90.0
29	c	0.55	0.30	1727 (sl)	93.0	91.0
30	c	0.30	0.65	1520 (sl)	90.0	90.0
31	c	0.60	0.30	1653 (sl)	96.0	96.0
32	c	0.40	0.50	1614 (sl)	97.3	97.4
33	c	0.70	0.20	1668 (sl)	97.3	97.4
34	c	0.65	0.15	1825 (sl)	97.3	97.4
35	c	0.35	0.50	1683 (sl)	97.3	97.4
36	c	0.45	0.40	1708 (sl)	96.0	96.0

ISBN: 84-699-5991-3 (http://www.cervantesvirtual.com/FichaObra.html?Ref=4845)

Table 2. *Results of the rigorous design method column design method. All cases work with a reflux ratio=2.*

Case	*Optimum D mol/h*	*$d(x_{Rcolumn}$ - $x_{Rbalance})$*	*No. Stages (Optimum location feed)*
1	60.0	0.00147	13.21 (6-7)
2	69.0	0.00027	11.98 (6-7)
3	50.5	0.00102	14.89 (7-8)
4	86.4	0.01709	10.24 (6-7)
5	69.8	0.01957	11.73 (6-7)
6	42.0	0.01333	9.02 (4-5)
7	69.4	0.00100	14.17 (8-9)
8	59.5	0.00190	12.79 (7-8)
9	59.7	0.00225	12.39 (6-7)
10	58.6	0.00251	7.10 (3-4)
11	69.2	0.00153	11.27 (6-7)
12	69.0	0.00013	8.00 (6-7)
13	52.1	0.00403	5.60 (3-4)
14	65.0	0.00320	7.79 (5-6)
15	83.6	0.00587	8.67 (5-6)
16	59.9	0.01281	4.80 (4-5)
17	68.8	0.00860	5.36 (4-5)
18	38.5	0.02657	3.67 (2-3)
19	68.8	0.00353	7.22 (5-6)
20	50.2	0.00436	7.83 (6-7)
21	78.6	0.00494	8.82 (6-7)
22	83.6	0.00506	9.57 (6-7)
23	50.3	0.00184	7.98 (6-7)
24	59.8	0.00187	6.96 (5-6)
25	60.0	0.00064	12.95 (6-7)
26	60.0	0.00231	14.84 (8-9)
27	60.0	0.00405	23.46 (13-14)
28	60.0	0.00084	12.95 (8-9)
29	69.0	0.00015	11.93 (5-6)
30	69.0	0.00124	12.79 (7-8)
31	69.0	0.00236	14.05 (9-10)
32	69.0	0.00223	15.84 (10-11)
33	69.0	0.00012	8.00 (5-6)
34	69.0	0.00416	8.25 (6-7)
35	69.0	0.0117	8.59 (7-8)
36	69.0	0.00515	8.63 (7-8)